Journal of
Materials in Life Sciences

Vol. 2 No. 2 (2023)

Full Paper

Biosorption of Methylene Blue on Sodium Hydroxide-Treated Oil Palm Trunk: Characterisation, Isotherm, and Kinetic Studies

Nurul Aqeelah Mohd Sakri[a], Waheeba Ahmed Al-Amrani[b], Haslizaidi Zakaria[a], Agustono Wibowo[a], Megat Ahmad Kamal Megat Hanafiah[a,*]

[a] Faculty of Applied Sciences, Universiti Teknologi MARA Pahang, 26400, Jengka, Pahang, Malaysia
[b] Department of Chemistry, College of Science, Ibb University, Ibb, Yemen

Article history
Received
13 September 2023
Revised
3 October 2023
Accepted
8 October 2023
Published online
25 November 2023

*Corresponding author
makmh@uitm.edu.my

Abstract

Methylene blue (MB), a commercial dye, is widely studied in ecology and environmental pollution research due to its toxic and carcinogenic properties. This work used a NaOH solution to treat oil palm trunk (SHOPT) as a biosorbent for MB removal under varied experimental settings. The SHOPT was characterised using FTIR, SEM-EDX, pH_{slurry}, and pH_{ZPC}.By using FTIR, functional groups like hydroxyl, carbonyl, and ether were found, which may have been the MB uptake's active sites. At pH 6, the highest biosorption capacity of 277.33 mg/g was predicted by the Langmuir isotherm model. SHOPT showed that MB had a greater biosorption capacity than other biosorbents. The desorption percentage recorded in neutral and acidic environments suggested the electrostatic attraction, π-π attraction, and H-bonding between MB molecules and the SHOPT surface. The results indicated that SHOPT might be a viable and practical biosorbent for eliminating MB from wastewater.

Keywords Biosorption, isotherm, kinetics, methylene blue, oil palm trunk

1.0 INTRODUCTION

Water resource contamination is a highly debated topic globally, given its potential to cause severe and fatal impacts on living organisms over extended periods. Dye effluents are a major cause for worry because of their toxicological and esthetic effects on a wide variety of organisms [Hamad and Idrus, 2022]. Synthetic dye, such as MB, is a common colourant in textile sectors and has exhibited environmental persistence, toxicity, carcinogenicity, and mutagenicity. A major consequence of the increasing use of industrial processes is the discharge of wastewater containing MB into surface water systems. It has been reported that MB can result in fatal serotonin poisoning in humans and aquatic wildlife when administered at dosages exceeding 5 mg/kg [Khan et al., 2022; Oladoye et al., 2022]. Thus, eliminating MB from wastewater is crucial to mitigate its adverse effects on the ecosystem.

Biosorption, a physicochemical treatment, has been thoroughly studied and recognised as an effective approach for eliminating MB. Since its introduction a few decades ago, the biosorption technique has increased by more than 100 percent [Hamad and Idrus, 2022]. Utilising biosorption as a wastewater treatment method is a straightforward process employing a plentiful and cost-effective biosorbent. This method substantially reduced the production of byproducts resulting from the oxidation or decomposition of MB. In addition, it displayed an exceptional ability to achieve a high MB removal efficiency [N'diaye et al., 2022]. Biosorbents that are ecologically sustainable and renewable, such as agricultural solid wastes comprising of organic compounds derived from leaves, trunks, and peels, are increasingly being utilised to eliminate MB from water [Liu et al., 2021; Misran et al., 2022; Nipa et al., 2023; Zein et al., 2023].

The palm oil industry is a significant agro-industry in Malaysia, producing a substantial amount of solid waste from oil palm (*Elaeis guineensis*) in the form of empty fruit bunches (OPEFB), leaves (OPL), fibres, fronds (OPF), and kernel shells

(PKS) [Setiabudi et al., 2016; Jasri et al., 2023]. These solid wastes are often left to decompose and have little economic value. Therefore, it would be advantageous from an environmental and financial standpoint to use oil palm solid wastes as a potentially low-cost biosorbent to remove MB. Numerous studies have examined the elimination of MB using OPL, OPF, and OPEFB. Jasri et al. [2023] recently reported MB removal using a mesoporous-activated carbon derived from OPF and PKS. The biosorbent showed a maximum biosorption capacity of 331.6 mg/g, according to the study. The kinetic data and the biosorption isotherm could be adequately explained by the Freundlich and pseudo-first-order (PFO) and pseudo-second-order (PSO) models, respectively. According to a different study, OPEFB was used as the natural precursor in the twofold carbonization and oxidation process to make reduced graphene oxide (rGO) [Ab Aziz et al., 2023]. The rGO exhibited a maximum biosorption capability of 50.07 mg/g. Activated carbons (AC) established from OPEFB and mesocarp fibres (MF) were able to remove acid orange 10 (AO10) and MB from watery-based solutions [Baloo et al., 2021]. The highest recorded biosorption capacities for AO10 and MB were 18.76 and 24.00 mg/g, respectively, under pH 3 and 2, an initial dye concentration of 50 mg/L, a biosorbent dose of 5 g/L, and a biosorption time of 90 min. Untreated OPL was utilised by Setiabudi et al. (2016) to remove MB from water. It was determined that the most favourable parameters for achieving a high removal rate of MB, specifically 88.72%, were a pH of 6, a biosorbent dose of 2.22 g/L, a temperature of 53°C, and an initial MB concentration of 259 mg/L. The Freundlich isotherm model best suited the experimental results, while the PSO kinetic model was observed to agree with the data. However, limited attention has been given to removing MB using OPT and its corresponding treatment. Mustikaningrum et al. (2020) and Miranda et al. (2021) performed a study on treating OPT with NaOH for obtaining nanocrystal cellulose (NCC). The work revealed that the treated OPT biosorbent exhibited effective removal of MB, with a percentage removal ranging between 69.46 and 72.51%. However, the study did not examine the optimal settings for conducting experiments, such as pH, biosorbent amount, pH_{ZPC}, the rate of reaction, and the isotherm. Thus, the current level of understanding regarding the biosorption of MB onto OPT treated with NaOH seems inadequate.

Based on the observations above, an investigation was conducted on the biosorption of MB utilising chemically-treated OPT by using a 0.10 M NaOH solution (SHOPT) under various experimental conditions in a batch mode. Treatment with NaOH helps to reduce lignin and convert the hydroxyl and carboxylic acid groups to alkoxide and carboxylate ions, which might improve the biosorption ability of a biosorbent. This study used an energy-dispersive X-ray spectrophotometer (EDX), a Fourier-transform infrared (FTIR) spectrophotometer, a scanning electron microscope (SEM), and an MB-laden biosorbent to characterise the biosorbent both before and after treatment. This study investigated the impact of some experimental parameters, including solution pH, biosorbent dose, and biosorption time. Kinetics and isotherm studies were conducted to learn more about the biosorption rate and the maximum amount of MB that can be adsorbed.

2.0 EXPERIMENTAL

2.1 Materials

An oil palm trunk (OPT) that was more than 25 years old and grew at the Universiti Teknologi MARA Pahang, Jengka Campus, Malaysia, was used as the source of a natural biosorbent for this experiment. The 98.5 percent pure cationic dye MB ($C_{16}H_{18}ClN_3S$, 319.86 g/mol) was purchased from HmbG Chemicals in Malaysia. In the biosorption studies, a stock solution of 1000 mg/L was prepared by dissolving 0.50 g of MB dye in 500 mL of distilled water. All of the chemical compounds utilised in the biosorption tests were of analytical grade quality without additional purification.

2.2 Preparation of Materials

To remove moisture, the middle section of the OPT was cut off, cleaned, and heated at 60°C for three days. To achieve 180-355 µm particles, the arid portion was manually chopped into pieces between 0.5 and 1.0 cm, crushed, and sieved. The sieved material was packed in a plastic container to keep moisture out before using the untreated OPT. At room temperature, 1 g of OPT was agitated for two hours in 100 mL of 0.10 M NaOH. Following treatment, OPT was given the moniker SHOPT after being rinsed ten times with 100 mL of distilled water and dried for two hours at 80°C in an oven.

2.3 Characterisation of Materials

Utilising an FTIR spectrophotometer (PerkinElmer Spectrum 100 FTIR, USA) from 4000 to 650 cm^{-1} and scanning electron microscopy (SEM) and energy dispersive X-ray spectroscopy (EDX) (EDX, Oxford Instrument, UK), the surface functional groups and surface morphology of OPT, SHOPT and MB-loaded SHOPT were identified, respectively. The surface charge of SHOPT was evaluated by pH_{slurry} and pH_{ZPC} approaches. The pH_{slurry} was ascertained by adding 0.10 g of SHOPT in 50 mL of distilled water. The blend was kept at a room temperature of 27°C for 24 h. The filtration process involved using a Whatman filter paper (No. 42), and subsequent measurement of the supernatant's pH was conducted using a pH meter. The following process was used to ascertain the pHZPC of the SHOPT: Conical flasks containing 50 mL (0.01 M) NaCl solutions were filled with initial pH (pHi) values ranging from 2 to 10. Next, for a full day, 0.50 g of SHOPT was magnetically stirred in 0.01 M NaCl solutions. Following filtration, the supernatant's final pH (pHf) was ascertained. In the plot of pHi-pHf versus pHi, the curve that intersected the pHi axis served as the representation of the pHZPC.

2.4 Biosorption-Desorption Studies

2.4.1 Batch MB Biosorption

MB dye solution (50 mL) was poured into a covered 100 mL conical Erlenmeyer flask and stirred at 300 rpm for the batch biosorption study. In order to evaluate the impact of solution pH and biosorbent dosage on the biosorption capability of SHOPT for a 25 mg/L MB dye solution, pH levels from 2 to 10 were used, and the SHOPT dosage was altered from 0.02 to 0.10 g, with a stirring time of 120 min. To adjust the pH of each solution, diluted 0.10 M NaOH or HCl was added. In a study on batch isotherm equilibrium experiments, starting with MB levels ranging from 25 to 125 mg/L, 0.02 g of SHOPT was varied with 50 mL of MB at pH 6. To perform kinetic analyses, a mixture was prepared by mixing 50 mL of pH 6 MB solutions with 0.02 g of SHOPT. The dye concentrations that were used were 5, 15, and 25 mg/L, and measurements were made at different times. The MB concentration was determined at a wavelength of 600 nm using a double-beam UV-visible spectrophotometer (UV-1800, Shimadzu, Japan) once equilibrium was reached. Equations (1) and (2) were utilised to determine the amount of MB adsorbed and the percentage of dye removal, respectively.

$$q_e = \frac{(C_o - C_e) \times V}{W} \quad (1)$$

$$\text{Removal (\%)} = \frac{C_o - C_e}{C_o} \times 100 \quad (2)$$

where q_e is the quantity of MB adsorbed (mg/g), C_o is an initial MB concentration (mg/L), C_e is MB dye equilibrium concentration (mg/L), W is the amount of SHOPT (g), and V is MB volume (L).

2.4.2 Desorption

When the biosorbent is no longer effective, it must be discarded, posing environmental risks. This study assessed the desorption capacity of MB-laden SHOPT under neutral and acidic conditions using distilled water and a dilute HCl solution. SHOPT was initially biosorbed with MB dye in the following manner: At a pH of 6, 0.02 g of SHOPT was introduced to a solution containing 50 mL of MB with a 25 mg/L concentration. The solution was stirred at a speed of 300 rpm, at a temperature of 300 K, for 120 min. The MB-laden SHOPT was separated through filtration and oven-dried at 60°C for 2 h. The remaining MB solution underwent spectroscopic analysis using a UV-visible spectrophotometer. The biosorbent was put in separate conical flasks with 50 mL distilled water or 0.01 M HCl solution as the eluent in order to desorb MB from the SHOPT surface. Equation (3) was used to determine the amount of MB desorbed after the mixture had been stirred for 30 minutes and filtered.

$$\text{Desorption efficiency (\%)} = \frac{\text{MB concentration after elution } (\frac{mg}{L})}{\text{MB concentration before elution } (\frac{mg}{L})} \times 100 \quad (3)$$

2.4.3 Statistical Analysis

To better match the experimental data to the intended models, a non-linear regression analysis of the isotherm and kinetic models using the Solver add-in was performed in Microsoft Excel. The statistical analyses used were the coefficient of determination (R^2) and the chi-square (χ^2), as shown by equations (4) and (5), respectively.

$$R^2 = \frac{\sum(q_{e,cal,i} - q_{e,exp,i})^2}{\sum(q_{e,cal,i} - q_{e,exp,avg})^2 - \sum(q_{e,cal.i} - q_{e,exp,i})^2} \quad (4)$$

$$\chi^2 = \sum_{i=1}^{N} \left| \frac{(q_{e,exp,i} - q_{e,cal,i})^2}{q_{e,exp,i}} \right| \quad (5)$$

where $q_{e,exp,i}$, $q_{e,calc,i}$, and $q_{e,exp,avg}$ are the observed and calculated MB concentration on SHOPT at any observation i, respectively, and N represents the observation number.

3.0 RESULTS AND DISCUSSION

3.1 Characterisation of SHOPT

3.1.1 FTIR Spectroscopy

FTIR spectroscopy facilitated the identification of the active functional groups of an adsorbent responsible for dye biosorption. The FTIR spectra for OPT, SHOPT, and MB-laden SHOPT are displayed in Figure 1. OPT has been known to be composed of lignocellulosic materials such as cellulose, hemicellulose, lignin components and others, made of functional groups including carboxylic acid, alkane, ester, aromatic, ether, ketone and alcohol [Abdul Khalil et al., 2008; Mustikaningrum et al., 2021]. The

peak at 3074 cm^{-1} in the OPT spectrum represented stretching vibration of the =C-H of the aromatic group while the peak in the range 3600 to 3200 cm^{-1} represented the O-H groups for cellulose, hemicelluloses, and lignin [Abdul Khalil et al., 2008]. A group of cellulose derivatives representing symmetric and asymmetric C-H saturated groups was found at 2832 and 2904 cm^{-1} in the FTIR spectra of OPT and SHOPT, respectively [Miranda et al., 2021]. The presence of the carboxylic acid group can be found by the broad peak between 2500 and 3600 cm^{-1}, and stretching vibrations of C-O and Si-O were seen between 1000 and 1200 cm^{-1}.

When comparing SHOPT with OPT, some peaks are lost or reduced in intensity in SHOPT. The peak at 1673 in OPT indicates the carbonyl stretching (C=O) associated with the carboxyl group or lignin. It has been observed that this peak decreased in intensity after the material reacted with NaOH. Moreover, the observation of a peak at 1420 cm^{-1} suggests that the C-H bending frequency of the carboxylic group in celluloses was weakened in SHOPT, likely due to the collapse of the cellulose structure. The peak intensity observed at 1602 cm^{-1}, corresponding to the C=C stretching of the aromatic chain in lignin, was reduced in the SHOPT spectrum. This indicates the collapse of the lignin structure. Upon the biosorption of MB onto SHOPT, there was a shift in absorption peak from 3335 to 3320 cm^{-1}, suggesting the attraction of MB molecules toward the RO^- group. Another important observation is a higher intensity peak at 1598 cm^{-1}, indicating that the C=C group originated from the aromatic rings of MB.

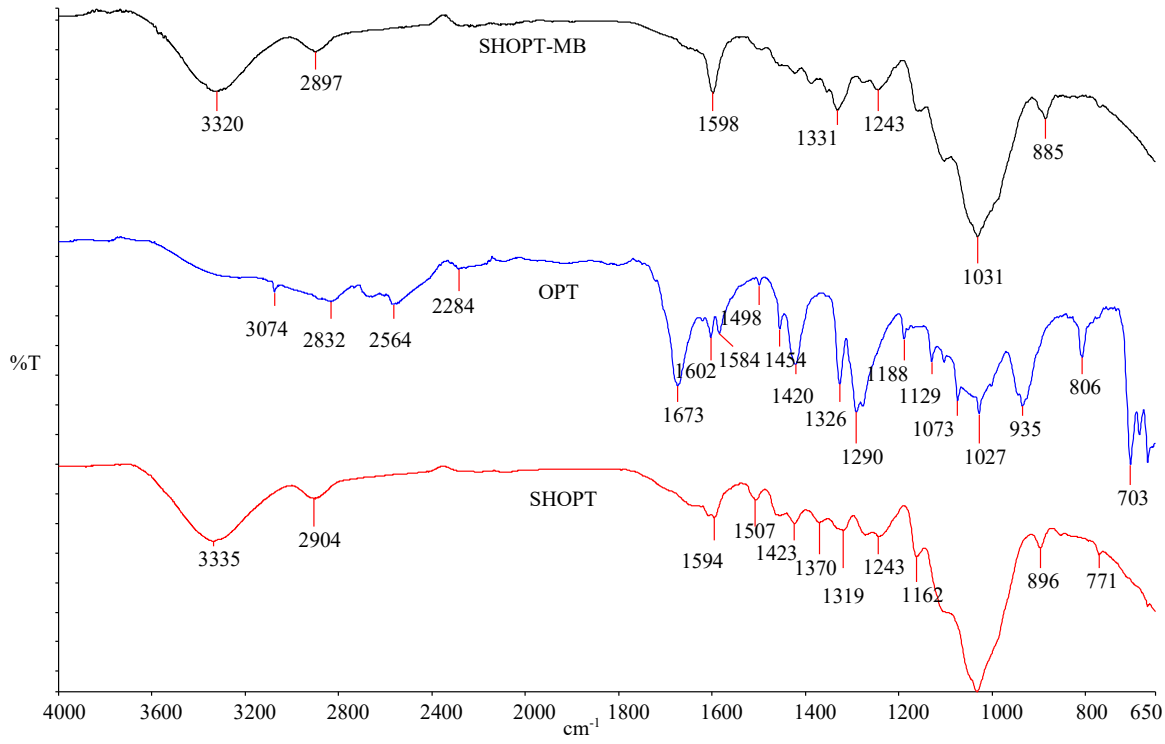

Figure 1 FTIR spectra for OPT, SHOPT and MB-laden SHOPT samples

3.1.2 SEM and EDX Analyses

The surface micrographs of SHOPT and MB-laden SHOPT, along with their corresponding EDX analyses, are presented in Figure 2(a-d) at a magnification of 700x. SHOPT displays a spongy, irregular shape with a lack of porous structure, possibly due to damage to the OPT cuticle during NaOH treatment [Zubair et al., 2020]. Biosorbent benefits from the surface's roughness and irregularity, letting the adsorbate easily stick to the active sites. Following the biosorption process, the surface of SHOPT that MB had adsorbed did not show much difference in surface morphology from unadsorbed SHOPT (Figure 2c), suggesting the physisorption through weak bonds. Figure 2(b) exhibits peaks for C and O in addition to peaks for macronutrients such as Mg, Ca, Na and (K. The biosorption process was evidenced by a distinct peak for sulphur (S) originating from MB, as shown in Figure 2(d). The loss of Na, K and Mg peaks after MB biosorption suggested the occurrence of an ion-exchange reaction.

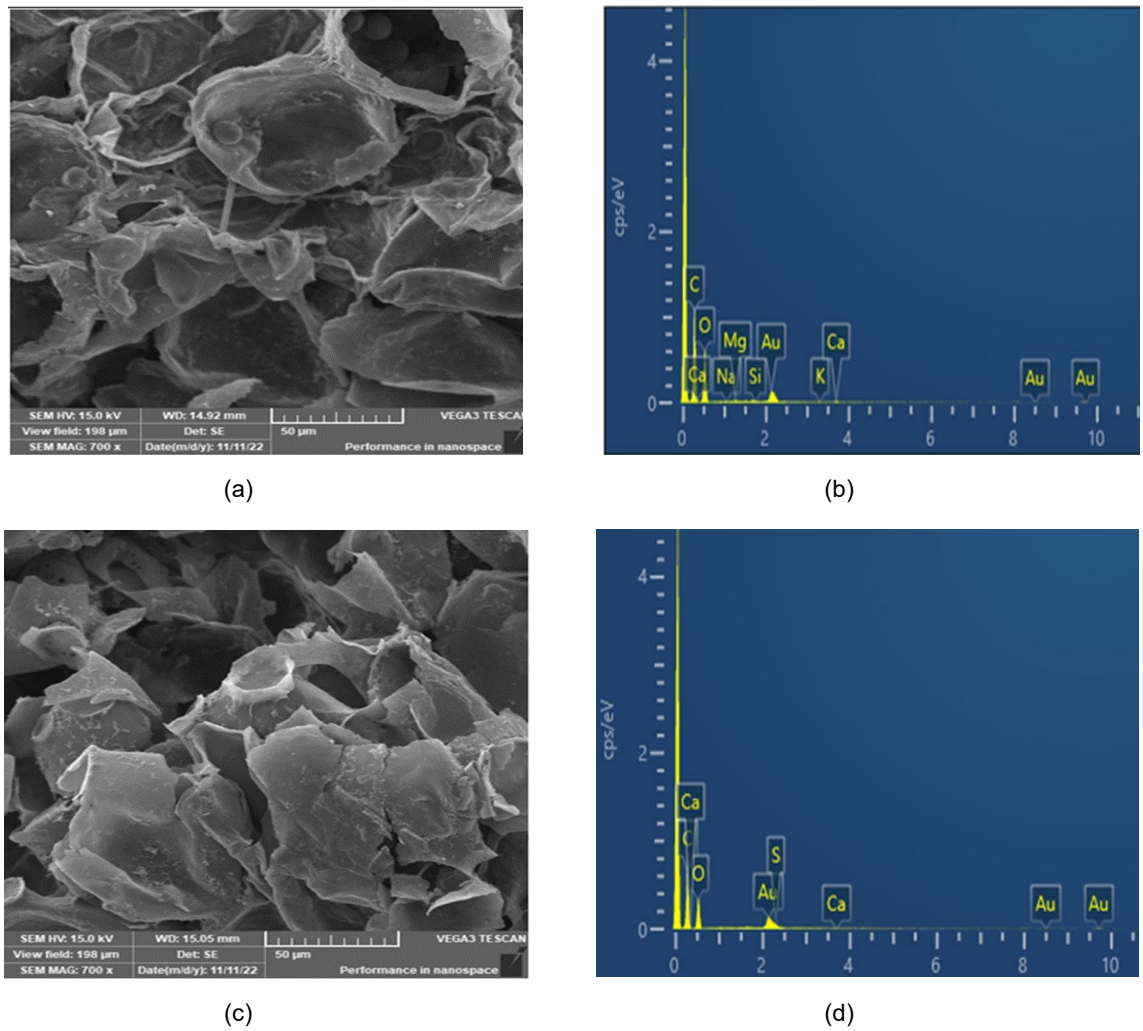

Figure 2 SEM images and EDX spectra of SHOPT (a and b) and MB-laden SHOPT (c and d), respectively.

3.1.3 Measurements of pH_{slurry} and pH_{ZPC}

The pH_{slurry} value of SHOPT was determined to be 6.44. Figure 3 displays a pH_{ZPC} plot with a recorded value of 6.07. The diverse functional groups such as O-H, RO^- and C=O, as shown by the FTIR spectrum (Figure 1), would increase the electrical attraction between the positively charged MB and the negatively charged SHOPT surface, increasing MB's biosorption at a pH higher than pH_{ZPC}.

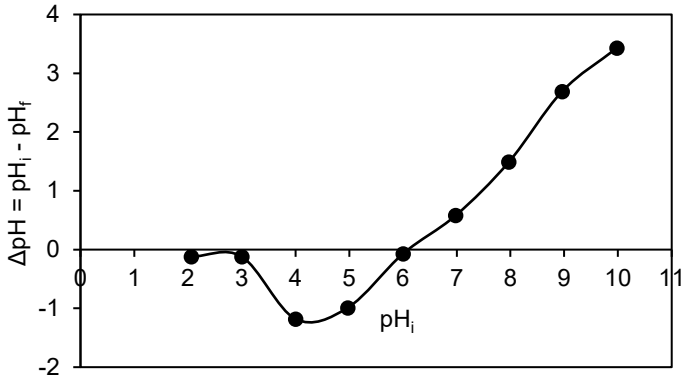

Figure 3 The pH_{ZPC} plot of SHOPT.

3.2 Batch Biosorption Performance of SHOPT

3.2.1 Initial MB Solution pH

A dye solution's acidity (pH) is a crucial biosorption parameter that significantly impacts the capacity of various biosorbents to adsorb dyes. This occurs because biosorbents profoundly affect dye molecules' ionisation and surface chemistry [Azoulay et al., 2020; Jasri et al., 2023]. The impact of varying the solution pH within the 2-10 on the process was investigated, and the outcomes are illustrated in Figure 4. As the pH was raised from 2 to 6, the electrostatic interaction between the negatively charged SHOPT surface ions and the positively charged MB molecules increased considerably. The biosorption capability of SHOPT towards MB molecules was observed to be small at low pH values. The observed phenomenon can be ascribed to the rise in the concentration of H_3O^+ ions within the bulk solution, which act as competitors with MB molecules for the active sites on the SHOPT. The results suggest that the biosorption process of MB onto SHOPT is significantly influenced by pH and exhibits a preference for mildly acidic environments. At pH values greater than 6, no significant changes were detected in the total amount of MB adsorbed onto the SHOPT surface. The observation above implies that the electrostatic attraction potentially influences the biosorption of MB onto SHOPT [Zubair et al., 2020]. Similar results were noted in the case of MB biosorption utilising other biosorbents, such as oil palm frond and palm leaves [Zeghoud et al., 2019], biochar-derived date palm frond waste [Zubair et al., 2020], sawdust palm oil [Esmaeili and Foroutan 2019] and fig leaf activated carbon [Al-Asadi and Al-Qaim 2023]. Consequently, a pH of 6 was selected for the ensuing analyses of kinetics and isotherms.

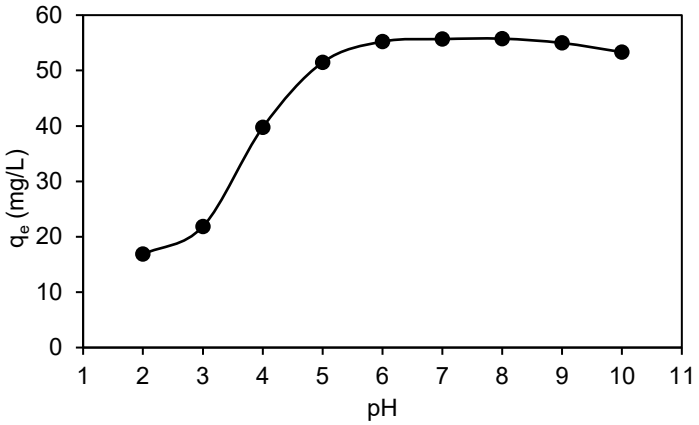

Figure 4 Effect of pH on MB biosorption onto SHOPT for 25 mg/L of initial MB at 120 min, 300 rpm, 0.02 g of biosorbent mass, and at 300 K.

3.2.2 SHOPT Dosages

The impact of varying biosorbent dosages of SHOPT on MB biosorption is exemplified in Figure 5. A notable decrease in biosorption capability was noted upon increasing the dosage of biosorbent from 0.02 to 0.10 g. The greater quantity of unsaturated active sites at higher biosorbent dosages is what causes the decrease in MB's capacity for biosorption, as explained in equation (1). In contrast, the percentage of MB removal exhibited an increase with the dosage of SHOPT, which can be ascribed to an elevation in the amount of available active groups for MB to get adsorbed. Other research in the literature review has revealed findings that are similar to these [Esmaeili and Foroutan, 2019; Liu et al., 2021; Nipa et al., 2023].

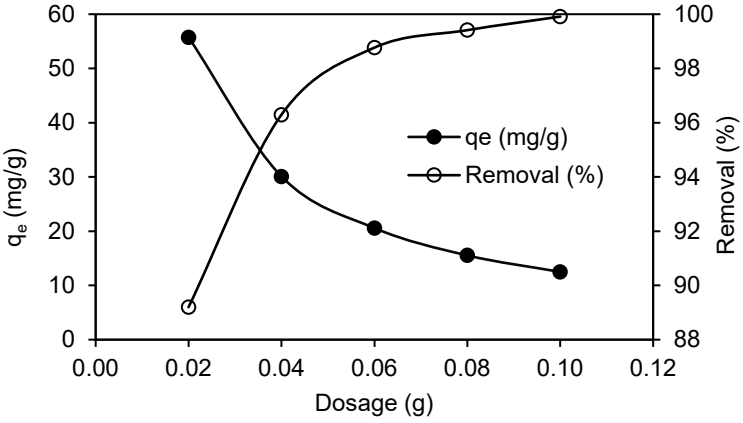

Figure 5 Impact of different SHOPT dosages on MB biosorption process for 25 mg/L of MB at 120 min, 300 rpm, pH 6, and at 300 K

3.2.3 Isotherm Studies

Figure 6 illustrates the relationship between the biosorption capacity (q_e, mg/g) and the equilibrium concentration of MB (C_e, mg/L). The trend that has been observed suggests that there is a beneficial relationship between the biosorption ability and the initial concentration of the MB solution. This correlation can be explained by the fact that the adsorbate mass transfer rate on the SHOPT is improved. As presented in Figure 6, the isotherm data for biosorption were analysed using the non-linear Langmuir [Langmuir 1918] and Freundlich [Freundlich 1926] isotherm models. The Langmuir model is predicated on the supposition of uniform biosorption within a monolayer, the absence of intermolecular contact among adsorbed species, and the absence of distinguishable biosorption locales. On the contrary, the Freundlich model (equation 7) assumes the occurrence of heterogeneous biosorption and multilayer biosorption.

$$q_e = \frac{q_{max} K_L C_e}{1 + K_L C_e} \quad (6)$$

$$q_e = K_F C_e^{\frac{1}{n}} \quad (7)$$

where maximum biosorption capacity is given by q_{max} (mg/g), the Langmuir constant (K_L) (L/mg) is related to binding energy, the Freundlich constant (K_F) (mg/g/(mg/L)$^{1/n}$) is the biosorption capacity, and n is the biosorption intensity.

The resulting values were compiled in Table 1, including the relevant statistical constants. According to Figure 6, the biosorption of MB demonstrated a higher degree of conformity to the Langmuir isotherm model than to the Freundlich isotherm model. Table 1 displays statistical metrics of goodness of fit, including a strong correlation coefficient (R^2=0.99) and a low chi value (χ^2 = 0.13). This shows that the dynamic sites on the SHOPT surface were uniform and that monolayer biosorption dominated the behaviour of the MB biosorption. Some other researchers have found similar outcomes [Nipa et al., 2023; Zein et al., 2023]. According to the Langmuir model, the biosorption capacity of SHOPT was 277.33 mg/g. This value indicates that SHOPT exhibits a greater biosorption capacity towards MB when compared to other renewable biosorbents documented in Table 2.

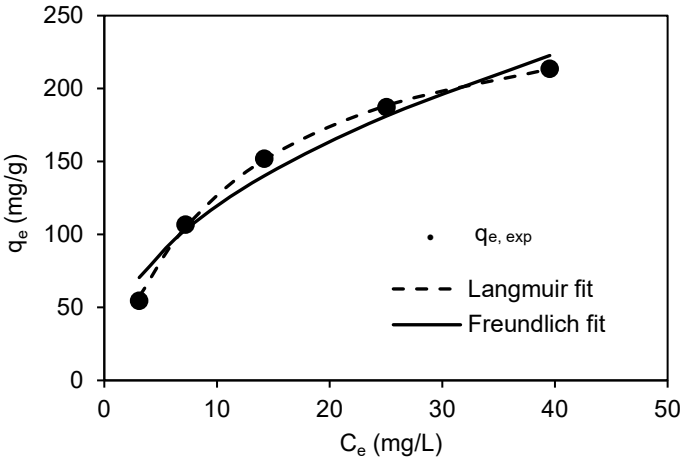

Figure 6 The non-linear Langmuir and Freundlich isotherm model fit experimental results of MB biosorption onto SHOPT at 25 to 125 mg/L, pH 6, 120 min., and at 27°C.

Table 1 SHOPT biosorbent MB biosorption isotherm constants.

Isotherm model	Parameters	Values
Langmuir	q_{max} (mg/g)	277.33
	K_L (L/mg)	0.091
	R^2	0.99
	χ^2	0.13
Freundlich	K_F [(mg/g)(L/mg)$^{1/n}$]	44.12
	n	0.44
	R^2	0.98
	χ^2	3.56

Table 2 Comparison of SHOPT biosorption capacity for MB with other biosorbents.

Biosorbent	pH	Time (min.)	Temp. (°C)	$q_{cal,\ max}$ (mg/g)	Reference
SHOPT	6	20	25	277.33	This study
Green microalgae (*Bracteacoccus sp*)	7	60	30	0.36	[Al-Fawwaz et al., 2023]
Grape leaves activated carbon	11	90	25	0.20	[Mousavi et al., 2022]
OPF-juice GSC	NA	1200	25	0.77	[Teow et al., 2020]
Mesocarp fibres (MF) of oil palm	2	90	25	24.00	[Baloo et al., 2021]
Mixture of palm waste	8	25	25	40.98	[Azoulay et al., 2020]
Reduced graphene oxide (rGO)	11	20	25	50.07	[Ab Aziz et al., 2023]
Sawdust of palm oil	8	120	25	53.95	[Esmaeili and Foroutan 2019]
Papaya bark fibre	11	720	27	66.67	[Nipa et al., 2023]
Fig leaf-activated carbon	11	60	25	69.93	[Al-Asadi and Al-Qaim 2023]
Palm frond base	6	50	25	70.87	[Zeghoud et al., 2019]
Palm leaflets		100		72.3	
Banana activated carbon	7	90	25	101.01	[Misran et al., 2022]
Oil palm (*Elaeis guineensis*) leaves	6	25	53	103.02	[Setiabudi et al., 2016]
Lemongrass leaves	9	90	25	112.35	[Zein et al., 2023]
Date palm fronds biochars	6	1440	25	206.61	[Zubair et al., 2020]
OPF activated carbon	10	20	25	331.6	[Jasri et al., 2023]

NA: Not available

3.2.4 Kinetic Studies

Comprehending the kinetics of biosorption holds paramount importance in ascertaining the suitable parameters for a batch operation on a large scale. Figure 7 illustrates the variations in the quantity of MB adsorbed on SHOPT over time, concerning three distinct initial MB concentrations of 5, 15, and 25 mg/L while maintaining a pH of 6. The initial five-minute period exhibited a swift rise in MB biosorption, suggesting that surface diffusion was the primary influential factor. The optimal biosorption capacity was attained after 20 min of the batch biosorption process. The models known as the pseudo-first-order (PFO) [Lagergren, 1898] (Eq. 8) and pseudo-second-order (PSO) [Ho and McKay, 1999] (Eq. 9) were applied to explore the rate of MB biosorption onto SHOPT.

$$q_t = q_e\,(1 - e^{k_1 t}) \qquad (8)$$

$$q_t = q_e^2 k_2 t/(1 + k_2 q_e t) \qquad (9)$$

The experimental results were fitted to the designated models, as depicted in Figure 7 (a-b), and the proposed constants and statistical coefficients are presented in Table 3. The PSO kinetics model demonstrated a satisfactory fit to the data, with higher R^2 values observed than the PFO kinetics model for all examined MB concentrations. Several additional studies utilising the analogues method have also indicated that biosorption of MB follows the PSO kinetics model [Setiabudi et al., 2016; Teow et al., 2020; Misran et al., 2022; Nipa et al., 2023].

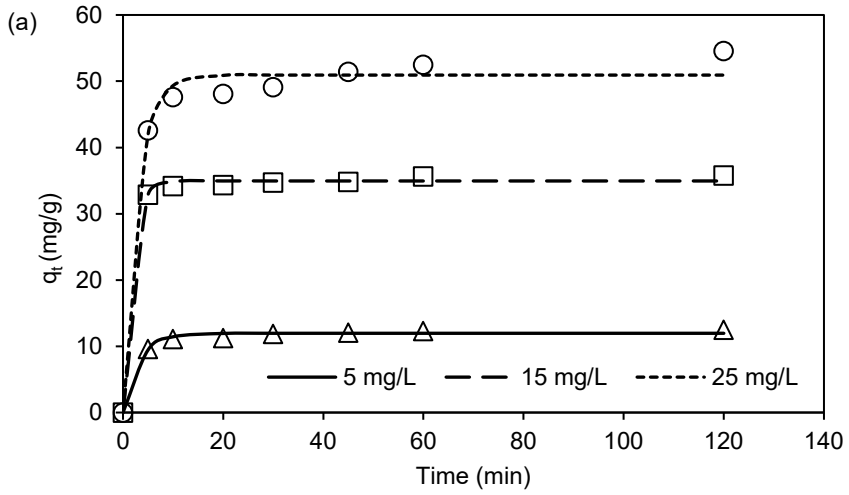

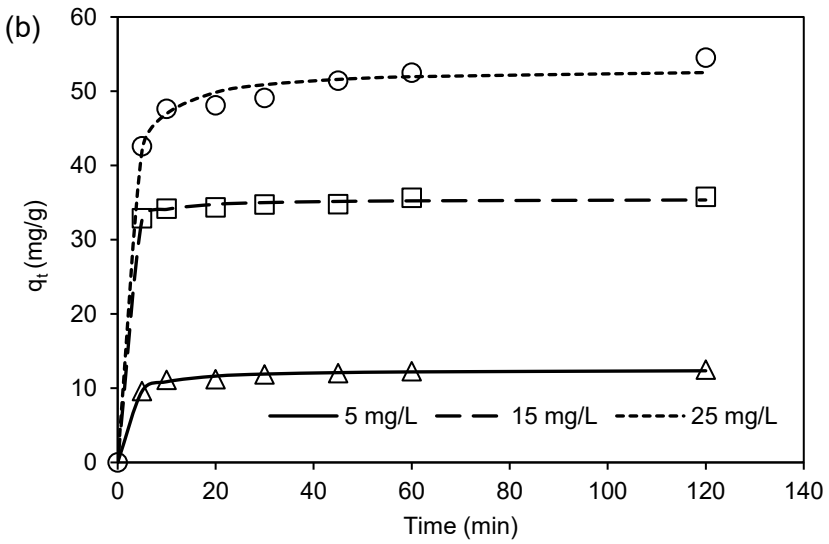

Figure 7 Non-linear fitting for biosorption kinetic models of (a) PFO and (b) PSO for the MB biosorption on SHOPT.

Table 3 Parameters of PFO and PSO kinetics models of MB biosorption onto SHOPT.

[MB] mg/L	PFO				PSO		
	q_{exp} (mg/g)	q_{cal} (mg/g)	k_1 (1/min)	R^2	k_2 (g/mg.min)	q_{cal} (mg/g)	R^2
5	12.50	11.96	0.31	0.82	0.05	12.49	0.95
15	35.80	34.95	0.56	0.64	0.07	35.47	0.87
25	54.55	50.93	0.35	0.67	0.02	53.08	0.99

3.2.5 Desorption

Table 4 presents the desorption proportion observed under neutral conditions using distilled water and an acidic solution with a concentration of 0.01 M HCl. The results indicate that distilled water could not desorb MB from the exhausted SHOPT, as evidenced by the zero desorption percentage. However, when subjected to 0.01 M HCl, the desorption percentage increased to 39.30%. The result has validated the robust contact between the MB molecules and the SHOPT biosorbent, thereby corroborating the FTIR spectra. A slight MB desorption found when 0.01 M HCl was used could suggest the weak interaction between MB and SHOPT, such as π-π interaction, electrostatic attraction and hydrogen bonding, and MB could be exchanged with protons from the acid.

Table 4 The biosorption-desorption percentage.

Distilled Water		0.01 M HCl	
Biosorption (%)	Desorption (%)	Biosorption (%)	Desorption (%)
90.03	0	90.03	39.30

4.0 CONCLUSION

The present investigation displayed that SHOPT exhibited promising potential as a biosorbent for eliminating cationic MB from aqueous solutions. The positive impact of SHOPT on the biosorption of MB can be attributed to its surface roughness and functional moieties, as revealed by SEM-EDX and FTIR analyses. The biosorption of MB onto SHOPT was significantly influenced by the pH of the solution within the pH range of 2 to 6. The optimal biosorption conditions were achieved at a pH value of 6 and a biosorbent dosage of 0.02 g. The Langmuir isotherm model demonstrated a satisfactory fit to the experimental data, while the PSO model exhibited a strong correlation with the kinetic of biosorption. Results from isotherm and desorption studies suggested the possibility of π-π stacking interaction, electrostatic attraction and hydrogen bonding between MB molecules and the SHOPT surface. The SHOPT biosorbent exhibits promising potential for removing MB from aqueous solutions due to its low-cost nature, abundance, and high removal of MB.

Acknowledgement

The authors would like to express their gratitude to the lab assistants who helped with the SEM-EDX study, as well as the Faculty of Applied Sciences at the Universiti Teknologi MARA Pahang campus for providing the facilities..

References

Ab Aziz, N. A. H., Md Ali, U. F., Ahmad, A. A., Mohamed Dzahir, M. I. H., Khamidun, M. H. and Abdullah, M. F. 2023. Non-functionalised oil palm waste-derived reduced graphene oxide for methylene blue removal: Isotherm, kinetics, thermodynamics, and mass transfer mechanism. Arabian Journal of Chemistry, 16, (1), 104387.

Abdul Khalil, H. P. S., Siti Alwani, M., Ridzuan, R., Kamarudin, H. and Khairul, A. 2008. Chemical composition, morphological characteristics, and cell wall structure of Malaysian oil palm fibers. Polymer-Plastics Technology and Engineering, 47, 273-280.

Al-Asadi, S. T. and Al-Qaim, F. F. 2023. Biosorption of methylene blue dye from aqueous solution using low cost adsorbent: Kinetic, isotherm biosorption and thermodynamic studies. Research square, 1-27.

Al-Fawwaz, A. T., Al Shra'ah, A. and Elhaddad, E. 2023. Bioremoval of methylene blue from aqueous solutions by green algae (Bracteacoccus sp.) isolated from North Jordan: Optimisation, kinetic, and isotherm studies. Sustainability, 15, (1), 842.

Azoulay, K., Bencheikh, I., Moufti, A., Dahchour, A., Mabrouki, J. and El Hajjaji, S. 2020. Comparative study between static and dynamic biosorption efficiency of dyes by the mixture of palm waste using the central composite design. Chemical Data Collections, 27, 100385.

Baloo, L., Isa, M. H., Sapari, N. B., Jagaba, A. H., Wei, L. J., Yavari, S., Razali, R. and Vasu, R. 2021. Adsorptive removal of methylene blue and acid orange 10 dyes from aqueous solutions using oil palm wastes-derived activated carbons. Alexandria Engineering Journal, 60, (6), 5611-5629.

Esmaeili, H. and Foroutan, R. 2019. Adsorptive behavior of methylene blue onto sawdust of sour lemon, date palm, and eucalyptus as agricultural wastes. Journal of Dispersion Science and Technology, 40, (7), 990-999.

Freundlich, H. 1926. Colloid and Capillary Chemistry. Methuen, Lon.

Hamad, H. N. and Idrus, S. 2022. Recent developments in the application of bio-waste-derived adsorbents for the removal of methylene blue from wastewater: A review. Polymers, 14, (4), 783.

Hameed, B. H. and El-Khaiary, M. I. 2008. Batch removal of malachite green from aqueous solutions by biosorption on oil palm trunk fibre: Equilibrium isotherms and kinetic studies. Journal of Hazardous Materials, 154, (1), 237-244.

Ho, Y.-S. and McKay, G. 1999. Pseudo-second order model for sorption processes. Process Biochem, 34, (5), 451–465.

Jasri, K., Abdulhameed, A. S., Jawad, A. H., Alothman, Z. A., Yousef, T. A. and Al Duaij, O. K. 2023. Mesoporous activated carbon produced from mixed wastes of oil palm frond and palm kernel shell using microwave radiation-assisted K_2CO_3 activation for methylene blue dye removal: Optimisation by response surface methodology. Diamond and Related Materials, 131, 109581.

Khan, I., Saeed, K., Zekker, I., Zhang, B., Hendi, A. H., Ahmad, A., Ahmad, S., Zada, N., Ahmad, H., Shah, L. A., Shah, T. and Khan, I. 2022. Review on Methylene Blue: Its properties, uses, toxicity and photodegradation. Water, 14, (2), 242.

Lagergren, S. K. 1898. About the theory of so-called biosorption of soluble substances. Sven Vetenskapsakad Handingar, 24, 1–39.

Langmuir, I. 1918. The biosorption of gases on plane surfaces of glass, mica and platinum. Journal of American Chemical Society, 40, 1361-1403.

Liu, X.-J., Li, M.-F. and Singh, S. K. 2021. Manganese-modified lignin biochar as adsorbent for removal of methylene blue. Journal of Materials Research and Technology, 12, 1434-1445.

Miranda, F. F., Putri, A. S., Mustikaningrum, M. and Yuliansyah, A. T. 2021. Preparation and characterisation of nano crystal cellulose from oil palm trunk for biosorption of methylene blue. AIP Conference Proceedings, 2338, 040008

Misran, E., Bani, O., Situmeang, E. M. and Purba, A. S. 2022. Banana stem based activated carbon as a low-cost adsorbent for methylene blue removal: Isotherm, kinetics, and reusability. Alexandria Engineering Journal, 61, (3), 1946-1955.

Mousavi, S. A., Mahmoudi, A., Amiri, S., Darvishi, P. and Noori, E. 2022. Methylene blue removal using grape leaves waste: optimisation and modeling. Applied Water Science, 12, (5), 112.

Mustikaningrum, M., Cahyono, R. B. and Yuliansyah, A. T. 2021. Effect of NaOH concentration in alkaline treatment process for producing nano crystal cellulose-based biosorbent for methylene blue. IOP Conference Series: Materials Science and Engineering, 1053, 012005

N'diaye, A. D., Kankou, M. S. A., Hammouti, B., Nandiyanto, A. B. D. and Al Husaeni, D. F. 2022. A review of biomaterial as an adsorbent: From the bibliometric literature review, the definition of dyes and adsorbent, the biosorption phenomena and isotherm models, factors affecting the biosorption process, to the use of typha species waste as adsorbent. Communications in Science and Technology, 7, (2), 140-153.

Nipa, S. T., Shefa, N. R., Parvin, S., Khatun, M. A., Alam, M. J., Chowdhury, S., Khan, M. A. R., Shawon, S. M. A. Z., Biswas, B. K. and Rahman, M. W. 2023. Biosorption of methylene blue on papaya bark fiber: Equilibrium, isotherm and kinetic perspectives. Results in Engineering, 17, 100857.

Oladoye, P. O., Ajiboye, T. O., Omotola, E. O. and Oyewola, O. J. 2022. Methylene blue dye: Toxicity and potential elimination technology from wastewater. Results in Engineering, 16, 100678.

Setiabudi, H. D., Jusoh, R., Suhaimi, S. F. R. M. and Masrur, S. F. 2016. Biosorption of methylene blue onto oil palm (*Elaeis guineensis*) leaves: Process optimisation, isotherm, kinetics and thermodynamic studies. Journal of the Taiwan Institute of Chemical Engineers, 63, 363-370.

Teow, Y. H., Tajudin, S. A., Ho, K. C. and Mohammad, A. W. 2020. Synthesis and characterisation of graphene shell composite from oil palm frond juice for the treatment of dye-containing wastewater. Journal of Water Process Engineering, 35, 101185.

Zeghoud, L., Gouamid, M., Ben Mya, O., Rebiai, A. and Saidi, M. 2019. Biosorption of methylene blue dye from aqueous solutions using two different parts of palm tree: palm frond base and palm leaflets. Water, Air, & Soil Pollution, 230, (8), 195.

Zein, R., Satrio Purnomo, J., Ramadhani, P., Safni, Alif, M. F. and Putri, C. N. 2023. Enhancing sorption capacity of methylene blue dye using solid waste of lemongrass biosorbent by modification method. Arabian Journal of Chemistry, 16, (2), 104480.

Zubair, M., Mu'azu, N. D., Jarrah, N., Blaisi, N. I., Aziz, H. A. and A. Al-Harthi, M. 2020. Biosorption behavior and mechanism of methylene blue, crystal violet, eriochrome black T, and methyl orange dyes onto biochar-derived date palm fronds waste produced at different pyrolysis conditions. Water, Air, & Soil Pollution, 231, (5), 240.